



**Theory of oblique-field magnetoresistance from spin centers in three-terminal spintronic devices**N. J. Harmon <sup>1,2,\*</sup> and M. E. Flatté <sup>1,3,†</sup><sup>1</sup>*Department of Physics and Astronomy, University of Iowa, Iowa City, Iowa 52242, USA*<sup>2</sup>*Department of Physics, University of Evansville, Evansville, Indiana 47722, USA*<sup>3</sup>*Department of Applied Physics, Eindhoven University of Technology, Eindhoven 5612 AZ, The Netherlands*

(Received 12 August 2020; accepted 13 January 2021; published 26 January 2021)

We present a general stochastic Liouville theory of electrical transport across a barrier between two conductors that occurs via sequential hopping through a single defect's spin-0 to spin-1/2 transition. We find magnetoconductances similar to Hanle features (pseudo Hanle features) that originate from Pauli blocking without spin accumulation, and also predict that evolution of the defect's spin modifies the conventional Hanle response, producing an inverted Hanle signal from spin center evolution. We propose studies in oblique magnetic fields that would unambiguously determine if a magnetoconductance results from spin-center assisted transport.

DOI: [10.1103/PhysRevB.103.035310](https://doi.org/10.1103/PhysRevB.103.035310)**I. INTRODUCTION**

A current flowing through a magnetic conductor, with carriers flowing into (spin injection) or out of (spin extraction) a nonmagnetic conductor, can produce a nonequilibrium spin population in the nonmagnetic material [1] that can be sensed through a spin-sensitive voltage. An applied magnetic field, intended to precess these nonequilibrium spins and thereby reduce the voltage (the Hanle effect or HE [2]), often produces surprising results challenging to interpret using reasonable spin coherence times [3–7]. Anomalous Hanle features (the inverted Hanle effect or IHE) were found with parallel applied field and magnetization; conventional interpretations attribute IHE to magnetic fringe fields from a nonuniform interface, however detailed structural measurements of the interface failed to correlate these features with measured nonuniformity. For currents and voltages measured using the same contact (three-terminal, or 3T measurements), features mimicking the HE and IHE were found [6,8], originating from magnetic-field-dependent transport through spin centers. However, agreement between some 3T and four-terminal (4T) nonlocal experiments indicates that the impurity effect does not always dominate over direct tunneling [9–11].

Here we analyze sequential spin-center-mediated tunneling between different magnetic or nonmagnetic leads in both the spin injection and spin extraction regimes using the stochastic Liouville equation (SLE) formalism. The SLE framework is highly adaptable to many physical systems, including spin-oriented tunneling through spin centers [12]. We apply the formalism to sequential tunneling involving a spin center that alternates between spin zero and spin one-half as its charge state changes. In the spin extraction regime, our formalism confirms previous studies that demonstrated supposed HE and IHE to be the result of a Pauli blockade [6,13], which we now refer to as “pseudo HE” and “pseudo IHE” phenomena.

To indicate the experimental geometry without assigning a mechanism we refer to “Hanle measurements” or “inverted Hanle measurements.” The combined effects of spin accumulation at the spin center and the coherent evolution of that spin accumulation lead to an altered spin injection process; we predict a previously undescribed, broad IHE (with same physical origin as the conventional HE) accompanying the known conventional HE (that can be broad or narrow). We will refer to these as “conventional HE” and “conventional IHE,” distinct from the pseudo HE and pseudo IHE. We analyze the oblique field data of Ref. [14] to show that a ratio of the angular dependent responses could, in principle, provide incontrovertible evidence of the impurity model by definitively ruling out the fringe-field mechanism for the inverted signal. Our calculations predict distinct magnetic field widths in the magnetoresponse that motivate further measurements to resolve the origin of the observed features. Lastly we show that the effects described herein *require charge current* and are thus not present for nonlocal (4T) measurements (or spin pumping).

**II. INTERFACIAL SPIN CENTERS**

This work treats spin injection and spin extraction between a nonmagnetic material (NM) and a ferromagnet (FM); the charge and/or spin current passes through an interfacial trap state through sequential hopping from one lead onto the trap, and then from the trap to the other lead. Figure 1(a) shows spin injection under a forward bias. The transition level of the spin center within the insulating barrier is labeled as  $(0/\frac{1}{2})$  to denote the two possible spin states: 0 here refers to the spin when no charge has hopped onto the level whereas  $\frac{1}{2}$  is the spin when a charged has hopped onto the level. Figure 1(b) shows the same center in the spin extraction regime (reverse bias, or with the nonmagnetic and ferromagnetic contacts reversed). We differentiate between the two configurations of Fig. 1 by defining (a) a *spin transport center* (since spin will accumulate in the NM) and (b) a *spin bottleneck center* since a bottleneck forms at the right junction. For both situations,

\*harmon.nicholas@gmail.com

†michael\_flatte@mailaps.org

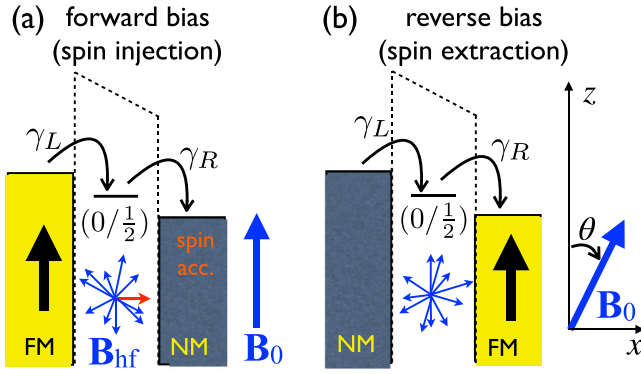


FIG. 1. Spin center-mediated transport between a ferromagnet (FM) and nonmagnetic metal (NM) for (a) spin injection and (b) spin extraction with interfacial spin centers possessing a transition level  $(0/\frac{1}{2})$ . The trap in (a) is a spin transport center. The trap in (b) is a spin bottleneck center. The IHE emerges from (a). If the spin center possesses a nuclear spin moment, assumed to be randomly oriented, some portion (red arrow in (a)) of the hyperfine field will be perpendicular to  $\mathbf{B}_0$ . This  $\perp \mathbf{B}_0$  component reduces the spin current; increasing  $B_0$  reduces the relative importance of  $B_{\text{hf}}$  which leads to increasing spin accumulation in the NM. (b) The applied magnetic field makes an angle  $\theta$  with respect to the  $z$  axis as shown in (b).

there are only the two designated spin states of the defect, differing by single charge carrier occupancy. The supplement discusses barrier traps with a transition level  $(\frac{1}{2}/0)$ , which under forward (reverse) bias yield charge and spin dynamics identical to the  $(0/\frac{1}{2})$  level under reverse (forward) bias [15]. Thus the spin and charge currents under forward bias, with both  $(0/\frac{1}{2})$  and  $(\frac{1}{2}/0)$  centers, are describable by the combined effects of the two configurations shown in Fig. 1, with  $N_t$  spin transport centers and  $N_b$  spin bottleneck centers. The total current is then

$$i_{\text{defect}} = N_t i_t(\mathbf{P}_L = \mathbf{P}, \mathbf{P}_R = 0) + N_b i_b(\mathbf{P}_L = \mathbf{P}, \mathbf{P}_R = 0), \\ = N_t i_t(\mathbf{P}_L = \mathbf{P}, \mathbf{P}_R = 0) + N_b i_t(\mathbf{P}_L = 0, \mathbf{P}_R = \mathbf{P}), \quad (1)$$

where  $i_{\text{defect}} = i_{\text{tot}} - i_{\text{dc}}$  is the difference between the total current  $i_{\text{tot}}$  and the direct (unaffected by the center) tunneling current  $i_{\text{dc}}$ . The bottleneck center/transport center current equivalency  $i_b(\mathbf{P}_L = \mathbf{P}, \mathbf{P}_R = 0) \equiv i_t(\mathbf{P}_L = 0, \mathbf{P}_R = \mathbf{P})$  is described in Ref. [15]. We concern ourselves only with  $i_{\text{defect}}$  so our goal is to calculate  $i_t(\mathbf{P}_L = \mathbf{P}, \mathbf{P}_R = 0)$  and  $i_t(\mathbf{P}_L = 0, \mathbf{P}_R = \mathbf{P})$ .  $\mathbf{P}_{L,R}$  are the carrier polarizations at the Fermi level in the leads.

### III. THEORY

Operators for the static magnetizations of each electrode are  $\hat{\mathbf{M}}_{L,R} = \frac{1}{2}(I + \mathbf{P}_{L,R} \cdot \boldsymbol{\sigma})$ . The time-evolution of the density matrix of the spin center,  $\rho(t)$ , is determined by the SLE. A  $2 \times 2$  matrix for the current  $\hat{i}$  fully describes the flow of charge and coherent spin. Diagonal elements represent the movement of charge with up or down spins, and off-diagonal elements describe the flow of charge with up and down spin superpositions. Charge currents are  $i = \text{Tr} \hat{i}$ , and spin currents are  $i_{s,L(R)} = \text{Tr} \hat{i}_{L(R)} \boldsymbol{\sigma}$ .

The current operators are formulated by identifying, e.g., in Fig. 1(b), the probability for a charge to pass from the barrier trap to the FM to be  $\frac{1}{2}(1 + \mathbf{P}_R \cdot \mathbf{P}_d(t))$ . The generalization of this probability for our current operator is  $\hat{\mathbf{M}}_R \rho(t)$  which yields, for the “right” current (trap to right lead  $R$ ) [12]

$$\hat{i}_R(t) = \frac{e}{2} \gamma_R \{\hat{\mathbf{M}}_R, \rho(t)\}, \quad (2)$$

where curly braces denote the anticommutator. The “left” current (left lead  $L$  to trap) is derived similarly after constraining the center to at most singly occupancy:

$$\hat{i}_L(t) = e \gamma_L [1 - \text{Tr} \rho(t)] \hat{\mathbf{M}}_L. \quad (3)$$

Charge conservation demands that the left charge current equal the right charge current.

Charge currents, spin currents, and spin accumulations are calculated from the spin center’s steady-state density matrix. The center undergoes several interwoven processes (e.g., charge hopping on and off, applied and local fields, charge and spin blocking) so unraveling the physics is not intuitive, however the SLE is well suited for this type of problem. It avoids complications from the choice of a spin quantization axis (see concluding remarks). The SLE [16–19]:

$$\frac{\partial \rho(t)}{\partial t} = \underbrace{-\frac{i}{\hbar} [\mathcal{H}, \rho(t)]}_{\text{coherent evolution}} - \underbrace{\gamma_R \{\hat{\mathbf{M}}_R, \rho(t)\}}_{\text{spin selection}} \\ + \underbrace{2\gamma_L [1 - \text{Tr} \rho(t)] \hat{\mathbf{M}}_L}_{\text{generation}}, \quad (4)$$

where  $\gamma_{R,L}$  are the spin dependent hopping rates to the right (left) electrode. The spin Hamiltonian at the spin center site is  $\mathcal{H} = \frac{\hbar}{2}(\mathbf{b}_0 + \mathbf{b}_{\text{hf}}) \cdot \boldsymbol{\sigma} = \frac{\hbar}{2} \mathbf{b} \cdot \boldsymbol{\sigma}$ , where  $\mathbf{b}_0 = g\mu_B \mathbf{B}_0 / \hbar$ ,  $\mathbf{b}_{\text{hf}} = g\mu_B \mathbf{B}_{\text{hf}} / \hbar$ ,  $\mathbf{b} = \mathbf{b}_0 + \mathbf{b}_{\text{hf}}$ ,  $\mathbf{B}_0$  is a uniform magnetic field, and  $\mathbf{B}_{\text{hf}}$  is the hyperfine field at the spin center. The hyperfine fields are assumed to be distributed as a Gaussian function with width  $\bar{b}_{\text{hf}}$ . The first term of the SLE represents the coherent evolution of the center’s spin, the second term denotes the spin-selective nature of tunneling into the FM. The third term describes hopping onto the impurity site from the left contact. These latter two terms are responsible for the stochastic nature of the SLE; they represent random hopping (with average rates  $\gamma_R$  and  $\gamma_L$ , respectively) from the center to the FM and from the NM to the center.

We assume the spin lifetimes and coherence times of the trap spin are longer than the transport processes producing the current.

#### A. Spin extraction

We now apply this theory to spin extraction [15] [Fig. 1(b)]. The current,

$$i \equiv i(\mathbf{P}_R, 0) = e \frac{(1 - P_R^2 \chi(\mathbf{b})) \gamma_L \gamma_R}{(1 - P_R^2 \chi(\mathbf{b})) \gamma_R + 2\gamma_L}, \quad (5)$$

with  $\chi(\mathbf{b}) = (\gamma_R^2 + (\mathbf{b} \cdot \hat{\mathbf{P}}_R)^2) / (\gamma_R^2 + b^2)$  agrees with Refs. [6,13], but differs from Ref. [20] (see concluding remarks).

The spin polarization of the impurities,  $\mathbf{P}_d = \text{Tr}(\sigma\rho)$ , is

$$\mathbf{P}_d = -\frac{2\gamma_L}{\gamma_R(1 - P_R^2\chi(\mathbf{b})) + 2\gamma_L} \times \frac{\gamma_R^2\mathbf{P}_R + \gamma_R\mathbf{b} \times \mathbf{P}_R + (\mathbf{b} \cdot \mathbf{P}_R)\mathbf{b}}{\gamma_R^2 + b^2}. \quad (6)$$

Spins parallel to the FM preferentially leave the barrier trap, thus a polarization opposite to the FM develops on the impurity site. This can be seen for  $\mathbf{b}_{\text{hf}} = 0$  and  $\mathbf{b}_0 \parallel \mathbf{P}_R$ , which leads to  $\mathbf{P}_d \propto -\mathbf{P}_R$ . This accumulation of defect spins, due to requiring spins leaving the defect to be parallel to  $\mathbf{P}_R$ , is called *spin filtering* [12]. There can be no spin accumulation in the NM since the impurity is only filled from the NM when it is empty; therefore no preferred spin is taken out of the NM [15].

### B. Spin injection

There is no spin filtering effect for the spin injection geometry [Fig. 1(a)], so the current,  $i(\mathbf{P}_L, \mathbf{P}_R = 0) = e\gamma_L\gamma_R/(\gamma_R + 2\gamma_L)$  is independent of  $\mathbf{b}_0$ . The steady state impurity spin polarization,

$$\mathbf{P}_d = \frac{2\gamma_L}{\gamma_R + 2\gamma_L} \left[ \frac{\gamma_R^2\mathbf{P}_L + \gamma_R\mathbf{b} \times \mathbf{P}_L + (\mathbf{b} \cdot \mathbf{P}_L)\mathbf{b}}{\gamma_R^2 + b^2} \right]. \quad (7)$$

The spin current,  $\mathbf{i}_s = e\gamma_R\mathbf{P}_d/2$ , leads to an excess (above an assumed unpolarized background) spin polarization of NM carriers per unit volume, which we call the spin accumulation density,  $\mathbf{p}_0$ , at the interface with area  $A$ . The spin accumulation density decays further within the NM as  $\mathbf{p} = \mathbf{p}_0 \exp(-x/\lambda_s)$ , where  $\lambda_s$  is the NM spin diffusion length. By setting the spin gained due to the spin current equal to the spin loss/evolution in NM [15],  $\mathbf{i}_s/e = A\lambda_s(\frac{1}{\tau_s}\mathbf{p}_0 - \mathbf{b}_0 \times \mathbf{p}_0)$ , the spin accumulation density can be solved analytically for a general spin current:

$$\mathbf{p}_0 = \frac{\tau_s}{A\lambda_s} \frac{\gamma_R\mathbf{P}_d + \tau_s\mathbf{b}_0 \times \mathbf{P}_d + \tau_s^2(\mathbf{b}_0 \cdot \mathbf{P}_d)\mathbf{b}_0}{2(1 + \tau_s^2b_0^2)}, \quad (8)$$

where the field dependence is hidden within  $\mathbf{P}_d$  [see Eq. (7)] and  $\tau_s$  is the spin relaxation time of carriers in the NM. This expression is identical to expressions for the oblique Hanle effect for direct tunneling, replacing the spin polarization injected into the NM with the defect polarization  $\mathbf{P}_d$  [21].

Canting the direction of the spin current away from the magnetization direction produces a previously unknown effective IHE. The origin of the canting is seen by investigating Eq. (7) for scenarios where  $\mathbf{b}_{\text{hf}} \parallel \mathbf{P}_L \parallel \mathbf{b}_0$  and  $\mathbf{b}_{\text{hf}} \perp \mathbf{P}_L \parallel \mathbf{b}_0$ . When  $\mathbf{b}_{\text{hf}} \parallel \mathbf{P}_L \parallel \mathbf{b}_0$ ,  $\mathbf{P}_d \parallel \mathbf{P}_L$  (i.e., no canting) and upon substituting Eq. (7) into Eq. (8) we find no field dependence. For  $\mathbf{b}_{\text{hf}} \perp \mathbf{P}_L \parallel \mathbf{b}_0$ ,  $\mathbf{P}_d$  develops components transverse to  $\mathbf{P}_L$  which indicate canting and the component of  $\mathbf{p} \parallel \mathbf{P}_L$  will be smaller than for a parallel hyperfine field. As the applied field is increased the transverse hyperfine component's effect is minimized and the maximum  $p_z$  is restored. This is an IHE but in reality its origin is the same as the conventional HE except that a ‘‘hidden’’ transverse field (a component of the hyperfine field  $\perp \mathbf{P}_L \parallel \mathbf{b}_0$ ) exists at the trap site. This transverse hyperfine component rotates the spin that is injected into the NM which results in a smaller accumulation of  $p_z$ . Prior theories

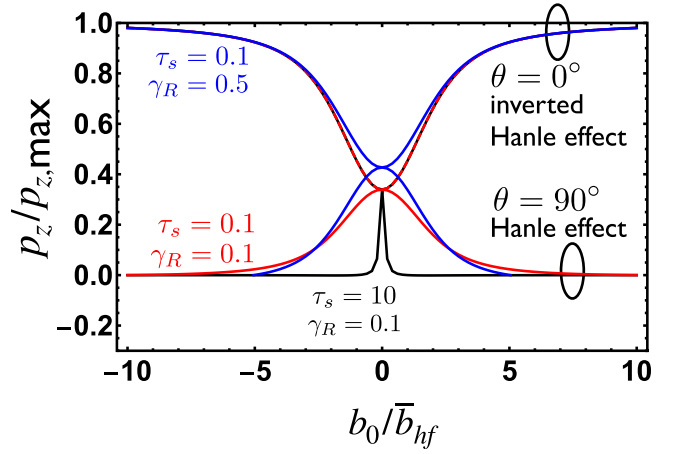


FIG. 2. Spin accumulation density parallel to  $\hat{z}$  in NM, for spin injection [see Fig. 1(a)], normalized to the maximum possible spin accumulation density,  $p_{z,\text{max}} = \gamma_L\gamma_R\tau_s/A\lambda_s(\gamma_R + 2\gamma_L)$ . The conventional Hanle (inverted Hanle) curves are concave down (up) and have widths sensitive (insensitive) to the spin relaxation time of carriers in the NM,  $\tau_s$ . Colors (red, blue, and black) denote different  $\tau_s$ 's and  $\gamma_R$ 's chosen in the calculation. The red curves are dashed to demonstrate that the red and black parameters yield almost identical inverted Hanle curves.  $\gamma_L = 10$  and all rates are in units of  $\bar{b}_{\text{hf}}$ .

of inverted Hanle measurements have either been (1) solely attributed to the spatially inhomogeneous fringe fields of the ferromagnetic contact [22], or (2) assigned to the pseudo IHE [6,8,13].

The hyperfine-field averaged NM spin accumulation is shown in Fig. 2. The combined dephasing evident in Eqs. (7) and (8) changes the conventional quadratic fall off in field to  $p_z \sim 1/(\gamma_R^2 + b^2)(1 + \tau_s^2b_0^2)$ . The width of the effects are primarily determined by  $\gamma_R$ ,  $\bar{b}_{\text{hf}}$ , or  $\tau_s^{-1}$ ; the width of the IHE is governed by the hyperfine field, and the HE by  $\tau_s^{-1}$  for  $\tau_s^{-1} \ll \bar{b}_{\text{hf}}$ , leading to very different widths. The discrepancy should offer a means of distinguishing if this trap-mediated spin accumulation leads to observed spin voltages. However, if  $\tau_s^{-1} \gg \bar{b}_{\text{hf}}$ , the widths are the same.

Experiments [11] on Fe/MgO/Si do observe a sharper peak of the HE superimposed upon a broader peak, and broader inverted Hanle peak. The spin lifetime of the narrow peak is comparable to the one obtained in an accompanying nonlocal four-terminal experiment, which suggests an origin in direct tunneling. The presence of similarly broad peaks in the Hanle and inverted Hanle curves point to additional charge hopping through spin bottleneck sites, though contributions from hopping through spin transport sites cannot be ruled out. Other experiments [23] on Fe/SiO<sub>2</sub>/Si displayed behavior in oblique fields which suggests the importance of stray fields.

### C. Oblique fields

Recently, the effect of oblique magnetic fields was measured to help distinguish spin accumulation and magnetic-field-dependent transport through barrier traps [14]. A strong field applied parallel to the magnetization suppresses any stray fields and returns the spin accumulation to its stray-field-free

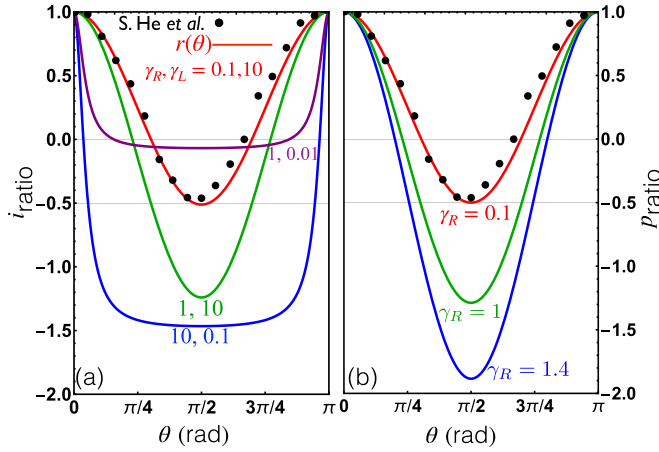


FIG. 3. (a)  $i_{\text{ratio}}$  and (b)  $p_{\text{ratio}}$  as a function of applied field angle for various hopping rates (labeling each curve) between the spin center level and a left NM contact and right FM contact. Black circles are data from Ref. [14]. (a)  $i_{\text{ratio}}$ 's (red, purple, green, and blue) are determined from numerically averaging over the gaussian distribution of hyperfine fields for  $i(0)$ . (b)  $p_{\text{ratio}}$ 's (black, green, and blue) are determined from Eq. (11), and are independent of  $\gamma_L$ . The red numerical line for  $\gamma_R = 0.1$ ,  $\gamma_L = 10$  is nearly identical to  $r(\theta) = \frac{3}{2} \cos^2 \theta - \frac{1}{2}$ .

value, which for oblique fields is proportional to  $\cos^2 \theta$  for direct tunneling [21]. Reference [14] compared oblique measurements (solid symbols in Fig. 3) to both the direct tunneling model and the trap model (spin bottleneck sites); the result was inconclusive as both models adequately described the data.

We propose alternate quantities to distinguish the two models: the ratio of the current or spin accumulation at zero and high fields at angle  $\theta$ . The barrier trap model predicts a universal response whereas the stray-field model depends on the details of the magnetic layer's roughness. Specifically,

$$i_{\text{ratio}} = \frac{\langle i(b_0 \rightarrow \infty, \theta) \rangle - \langle i(b_0 = 0) \rangle}{\langle i(b_0 \rightarrow \infty, \theta = 0^\circ) \rangle - \langle i(b_0 = 0) \rangle} \quad (9)$$

for spin extraction and

$$p_{\text{ratio}} = \frac{\langle p_z(b_0 \rightarrow \infty, \theta) \rangle - \langle p_z(b_0 = 0) \rangle}{\langle p_z(b_0 \rightarrow \infty, \theta = 0^\circ) \rangle - \langle p_z(b_0 = 0) \rangle} \quad (10)$$

for spin injection. Angular brackets denote averaging over the gaussian distribution of hyperfine fields.

In general,  $i_{\text{ratio}}$  can only be computed numerically but  $p_{\text{ratio}}$  is analytically found to be [15]

$$p_{\text{ratio}} = \frac{3C(\cos^2 \theta - 1)}{2} + 1 \quad (11)$$

with

$$C = \left[ 1 - \frac{\gamma_R^2}{b_{\text{hf}}^2} + \frac{\sqrt{2\pi}}{2} \frac{\gamma_R^3}{b_{\text{hf}}^3} e^{\gamma_R^2/2b_{\text{hf}}^2} \text{erfc}\left(\frac{1}{\sqrt{2}} \frac{\gamma_R}{b_{\text{hf}}}\right) \right]^{-1}, \quad (12)$$

where remarkably, there is no dependence on  $\gamma_L$  nor  $\tau_s$ , and no approximations have been made on the relative size of the various rates. Meanwhile  $i_{\text{ratio}}$  is independent of  $\tau_s$ . As shown in the Supplement Material [15], for either metric, if

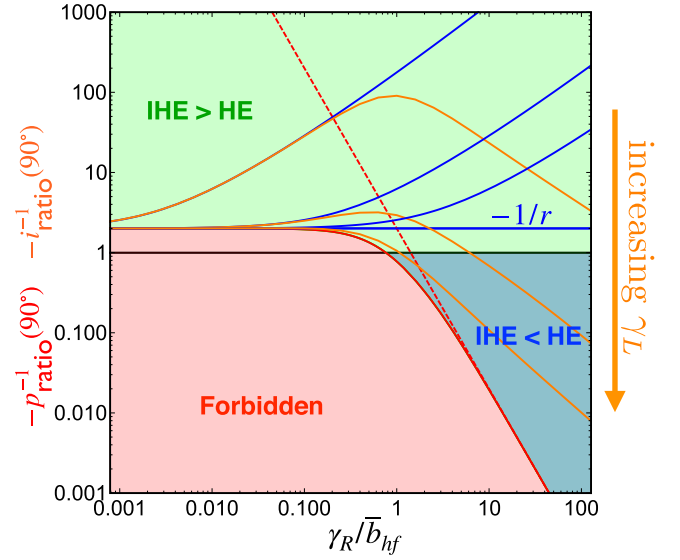


FIG. 4. Ratio of the inverted Hanle effect (IHE) to the Hanle effect (HE) absolute scale factors versus  $\gamma_R$  for either spin extraction (orange, current ratio) or spin injection (red, polarization ratio). Blue curves are for  $\gamma_R \ll \bar{b}_{\text{hf}}$  with the horizontal blue line =  $-r^{-1}(\theta)$ . The dashed red line =  $2\bar{b}_{\text{hf}}^2 \csc \theta / \gamma_R^2$ . Values of  $\gamma_L$  are 0.001, 0.1, 1. As  $\gamma_L$  increases further, the orange lines converges to the red line.  $p_{\text{ratio}}$  is independent of  $\gamma_L$ .

$\gamma_R \ll \bar{b}_{\text{hf}} \ll \gamma_L$  then  $i_{\text{ratio}} = p_{\text{ratio}} \equiv r(\theta) = (3 \cos^2 \theta - 1)/2$ . Figure 3 shows the oblique field data from Ref. [14], along with  $r(\theta)$ , and the agreement with the barrier trap prediction is remarkable. The fixed ratio between currents at  $90^\circ$  and  $0^\circ$  [ $r(90^\circ) = -1/2$ ] was already noted in STO/LAO/Co structures [6]. Ratios near this value hold in some other experiments as well, but not all [5,24,25]. The common occurrence of the ratio is a strong indicator that stray fields rarely are the IHE mechanism. Different structures and magnets possess varying degrees of roughness and thus varying stray field distribution which have no cause to yield  $r(90^\circ) = -1/2$ .

Distinguishing spin transport centers from spin bottleneck centers is difficult solely from the angle-dependent amplitudes. The width for spin bottleneck centers, determined by the hyperfine coupling, is the same for parallel and perpendicular applied fields [15]. This is not the case for spin transport centers when  $\tau_s \bar{b}_{\text{hf}} \gg 1$ ; in this instance, the width is governed by  $\tau_s^{-1}$ . We expect that both impurity types occur (in addition to direct tunneling) so disentangling their contributions in measurements in the literature is not feasible within the scope of this paper. For  $\gamma_R \ll \bar{b}_{\text{hf}} \ll \gamma_L$ , both  $i_{\text{ratio}}$  and  $p_{\text{ratio}}$  approach  $r$  but outside that strict constraint the two ratios are not identical [Fig. 3(a) versus Fig. 3(b)].  $p_{\text{ratio}}$  is more sensitive to  $\gamma_R$  than  $i_{\text{ratio}}$ .

Figure 4 summarizes the magnitudes of the conventional and pseudo HE and IHE for either spin injection (red) or spin extraction (orange). The blue curves (red dashed line) indicate slow (fast)  $\gamma_R$  approximations for extraction (injection). Three regions are represented by red (forbidden), cyan (IHE < HE), and green (IHE > HE). The quantity  $-x_{\text{ratio}}^{-1}(90^\circ)$  should be interpreted as the ratio between IHE and HE: e.g.  $-i_{\text{ratio}}^{-1}(90^\circ) = \Delta i(\theta = 0^\circ) / \Delta i(\theta = 90^\circ)$ . The large- $\gamma_R$  asymptotic behavior

of  $-p_{\text{ratio}}^{-1}(\theta)$  is  $2\bar{b}_{\text{hf}}^2 \csc \theta / \gamma_R^2$  which is the dashed red line in Fig. 4.

#### IV. RAMIFICATIONS FOR NONLOCAL SPIN DETECTION

For smaller voltage bias, hops occur back and forth between each lead and the barrier trap. At zero bias (zero charge current), no spin current is produced [15]. Thus the described magnet effects for spin transport centers or spin bottleneck centers cannot occur without a bias, so such effects are not expected in nonlocal measurements. Reference [11] observes impurity-assisted signatures in three-terminal but not four-terminal devices. Thus the trap effects here will not confuse spin pumping or thermal spin transport experiments involving FM/NM interfaces without charge currents. The traps will not alter the spin currents without charge currents, nor can unbiased spin centers mediate ferromagnetic proximity polarization [26–28].

#### V. CONCLUDING REMARKS

The ambiguity in the spin-dependent magnetoresistance in a resonant tunneling formulation originates from the dependence of the Hubbard Hamiltonian ( $Un_{\uparrow}n_{\downarrow}$ ) on the spin quantization axis [13,20]. Our results are independent of the quantization axis and agree with Ref. [13], although the reason why this is the “proper” choice is unclear; we thus suggest the SLE approach is more robust as no assumption of an axis is required.

#### ACKNOWLEDGMENTS

The solution of these problems, comparison with experiment, and key results were supported by the U. S. Department of Energy, Office of Science, Office of Basic Energy Sciences, under Award No. DE-SC0016379. The formulation of this problem and initial results were supported in part by C-SPIN, one of six centers of STARnet, a Semiconductor Research Corporation program, sponsored by MARCO and DARPA.

- 
- [1] M. Johnson and R. H. Silsbee, Interfacial Charge-Spin Coupling: Injection and Detection of Spin Magnetization in Metals, *Phys. Rev. Lett.* **55**, 1790 (1985).
- [2] M. Johnson and R. H. Silsbee, Spin-injection experiment, *Phys. Rev. B* **37**, 5326 (1988).
- [3] M. Tran, H. Jaffres, C. Deranlot, J. M. George, A. Fert, A. Miard, and A. Lemaitre, Enhancement of the Spin Accumulation at the Interface between a Spin Polarized Tunnel Junction and a Semiconductor, *Phys. Rev. Lett.* **102**, 036601 (2009).
- [4] R. Jansen, S. P. Dash, S. Sharma, and B. C. Min, Silicon spintronics with ferromagnetic tunnel devices, *Semicond. Sci. Technol.* **27**, 083001 (2012).
- [5] O. Txoperena, M. Gobbi, A. Bedoya-Pinto, F. Golmar, X. Sun, L. E. Hueso, and F. Casanova, How reliable are Hanle measurements in metals in a three-terminal geometry? *Appl. Phys. Lett.* **102**, 192406 (2013).
- [6] H. Inoue, A. G. Swartz, N. J. Harmon, T. Tachikawa, Y. Hikita, M. E. Flatté, and H. Y. Hwang, Origin of the Magnetoresistance in Oxide Tunnel Junctions Determined through Electric Polarization Control of the Interface, *Phys. Rev. X* **5**, 041023 (2015).
- [7] O. Txoperena and F. Casanova, Spin injection and local magnetoresistance effects in three-terminal devices, *J. Phys. D: Appl. Phys.* **49**, 133001 (2016).
- [8] O. Txoperena, Y. Song, L. Qing, M. Gobbi, L. E. Hueso, H. Dery, and F. Casanova, Impurity-Assisted Tunneling Magnetoresistance under a Weak Magnetic Field, *Phys. Rev. Lett.* **113**, 146601 (2014).
- [9] X. Lou, C. Adelman, M. Furis, S. A. Crooker, C. J. Palmström, and P. A. Crowell, Electrical Detection of Spin Accumulation at a Ferromagnet-Semiconductor Interface, *Phys. Rev. Lett.* **96**, 176603 (2006).
- [10] X. Lou, C. Adelman, S. A. Crooker, E. S. Garlid, J. Zhang, K. S. Madhukar Reddy, S. D. Flexner, C. J. Palmström, and P. A. Crowell, Electrical detection of spin transport in lateral ferromagnet-semiconductor devices, *Nat. Phys.* **3**, 197 (2007).
- [11] Y. Aoki, M. Kamen, Y. Ando, E. Shikoh, Y. Suzuki, T. Shinjo, M. Shiraishi, T. Sasaki, T. Oikawa, and T. Suzuki, Investigation of the inverted Hanle effect in highly doped Si, *Phys. Rev. B* **86**, 081201(R) (2012).
- [12] N. J. Harmon and M. E. Flatté, Theory of spin-coherent electrical transport through a defect spin state in a metal / insulator / ferromagnet tunnel junction undergoing ferromagnetic resonance, *Phys. Rev. B* **98**, 035412 (2018).
- [13] Y. Song and H. Dery, Magnetic-Field-Modulated Resonant Tunneling in Ferromagnetic-Insulator-Nonmagnetic Junctions, *Phys. Rev. Lett.* **113**, 047205 (2014).
- [14] S. He, J.-H. Lee, P. Grünberg, and B. K. Cho, Angular variation of oblique Hanle effect in CoFe/SiO<sub>2</sub>/Si and CoFe/Ta/SiO<sub>2</sub>/Si tunnel contacts, *J. Appl. Phys.* **119**, 113902 (2016).
- [15] See Supplemental Material at <http://link.aps.org/supplemental/10.1103/PhysRevB.103.035310> for further description of spin centers in spin injection and extraction regimes, details of the Hanle effect calculation, additional results for spin extraction regime, details on the calculations of  $i_{\text{ratio}}$  and  $p_{\text{ratio}}$ , and analysis of the junction with zero bias which is relevant for nonlocal spin detection techniques.
- [16] R. Kubo, Stochastic Liouville equations, *J. Math. Phys.* **4**, 174 (1963).
- [17] R. Kubo, in *Stochastic Processes in Chemical Physics*, edited by K. E. Shuler (Wiley, New York, 1969), Chap. 6, A Stochastic Theory of Line Shape, p. 101.
- [18] R. Haberkorn, Density matrix description of spin-selective radical pair reactions, *Mol. Phys.* **32**, 1491 (1976).
- [19] R. Haberkorn and W. Dietz, Theory of spin-dependent recombination in semiconductors, *Solid State Commun.* **35**, 505 (1980).
- [20] Z. Yue, M. C. Prestgard, A. Tiwari, and M. E. Raikh, Resonant magnetotunneling between normal and ferromagnetic electrodes in relation to the three-terminal spin transport, *Phys. Rev. B* **91**, 195316 (2015).
- [21] F. Meier and B. P. Zacharenya, *Optical Orientation: Modern Problems in Condensed Matter Science* (North-Holland, Amsterdam, 1984), Vol. 8.

- [22] S. P. Dash, S. Sharma, J. C. Le Breton, J. Peiro, H. Jaffrès, J.-M. George, A. Lemaître, and R. Jansen, Spin precession and inverted Hanle effect in a semiconductor near a finite-roughness ferromagnetic interface, *Phys. Rev. B* **84**, 054410 (2011).
- [23] S. Sato, R. Nakane, and M. Tanaka, Origin of the broad three-terminal Hanle signals in Fe/SiO<sub>2</sub>/Si tunnel junctions, *Appl. Phys. Lett.* **107**, 032407 (2015).
- [24] A. Jain, J.-C. Rojas-Sanchez, M. Cubukcu, J. Peiro, J. C. Le Breton, E. Prestat, C. Vergnaud, L. Louahadj, C. Portemont, C. Ducruet, V. Baltz, A. Barski, P. Bayle-Guillemaud, L. Vila, J.-P. Attané, E. Augendre, G. Desfonds, S. Gambarelli, H. Jaffrès, J.-M. George, and M. Jamet, Crossover from Spin Accumulation into Interface States to Spin Injection in the Germanium Conduction Band, *Phys. Rev. Lett.* **109**, 106603 (2012).
- [25] H. N. Tinkey, P. Li, and I. Appelbaum, Inelastic electron tunneling spectroscopy of local spin accumulation devices, *Appl. Phys. Lett.* **104**, 232410 (2014).
- [26] R. K. Kawakami, Y. Kato, M. Hanson, I. Malajovich, J. M. Stephens, E. Johnston-Halperin, G. Salis, A. C. Gossard, and D. D. Awschalom, Ferromagnetic imprinting of nuclear spins in semiconductors, *Science* **294**, 131 (2001).
- [27] C. Ciuti, J. P. McGuire, and L. Sham, Spin Polarization of Semiconductor Carriers by Reflection off a Ferromagnet, *Phys. Rev. Lett.* **89**, 156601 (2002).
- [28] Y.-S. Ou, Y.-H. Chiu, N. J. Harmon, P. Odenthal, M. Sheffield, M. Chilcote, R. K. Kawakami, and M. E. Flatté, Exchange-Driven Spin Relaxation in Ferromagnet-Oxide-Semiconductor Heterostructures, *Phys. Rev. Lett.* **116**, 107201 (2016).